X-Box Binding Protein 1 Is Essential for Insulin Regulation of Pancreatic α-Cell Function

X-Box Binding Protein 1 Is Essential for Insulin Regulation of Pancreatic α-Cell Function

Masaru Akiyama,[1] Chong Wee Liew,[1,3] Shusheng Lu,[2] Jiang Hu,[1] Rachael Martinez,[1] Ben Hambro,[1] Robert T. Kennedy,[2] and Rohit N. Kulkarni[1]

Patients with type 2 diabetes (T2D) often exhibit hyperglucagonemia despite hyperglycemia, implicating defective α-cell function. Although endoplasmic reticulum (ER) stress has been suggested to underlie β-cell dysfunction in T2D, its role in α-cell biology remains unclear. X-box binding protein 1 (XBP1) is a transcription factor that plays a crucial role in the unfolded protein response (UPR), and its deficiency in β-cells has been reported to impair insulin secretion, leading to glucose intolerance. To evaluate the role of XBP1 in α-cells, we created complementary in vivo (α-cell–specific XBP1 knockout [αXBPKO] mice) and in vitro (stable XBP1 knockdown α-cell line [αXBPKD]) models. The αXBPKO mice exhibited glucose intolerance, mild insulin resistance, and an inability to suppress glucagon secretion after glucose stimulation. αXBPKD cells exhibited activation of inositol-requiring enzyme 1, an upstream activator of XBP1, leading to phosphorylation of Jun NH_2-terminal kinase. Interestingly, insulin treatment of αXBPKD cells reduced tyrosine phosphorylation of insulin receptor substrate 1 (IRS1) (pY^{896}) and phosphorylation of Akt while enhancing serine phosphorylation (pS^{307}) of IRS1. Consequently, the αXBPKD cells exhibited blunted suppression of glucagon secretion after insulin treatment in the presence of high glucose. Together, these data indicate that XBP1 deficiency in pancreatic α-cells induces altered insulin signaling and dysfunctional glucagon secretion. ***Diabetes*** **62:2439–2449, 2013**

In addition to the defects in β-cell secretory function and reduced β-cell mass, patients with type 2 diabetes (T2D) frequently manifest hyperglucagonemia that contributes to uncontrolled hyperglycemia (1–3). Although it is generally accepted that α-cell dysfunction is a feature of overt T2D, the mechanism(s) that contribute to the hypersecretion by α-cells is not fully understood. In addition to glucose (4), we and others have reported that insulin signaling in α-cells plays a critical role in the regulation of glucagon secretion and that impaired insulin signaling in α-cells leads to a diabetic phenotype due to enhanced glucagon secretion (5,6). Further, the α-cell has been suggested to be regulated by other intraislet paracrine factors, such as somatostatin (7), γ-aminobutyric acid (GABA) (8), and zinc ions (Zn^{2+}) (9), in addition to insulin.

From the [1]Section of Islet Cell Biology and Regenerative Medicine, Joslin Diabetes Center and Harvard Medical School, Boston, Massachusetts; the [2]Departments of Chemistry and Pharmacology, University of Michigan, Ann Arbor, Michigan; and the [3]Department of Physiology and Biophysics, University of Illinois at Chicago, Chicago, Illinois.
Corresponding author: Rohit N. Kulkarni, rohit.kulkarni@joslin.harvard.edu.
Received 13 December 2012 and accepted 8 March 2013.
DOI: 10.2337/db12-1747

A notable feature in patients with T2D is a gradual loss of β-cell mass while their α-cell mass is maintained relatively intact (10). Although hyperglycemia, elevated free fatty acids (11), oxidative stress, and endoplasmic reticulum (ER) stress (12,13) have all been proposed to contribute to the reduced β-cell mass, the mechanisms that underlie the relative refractoriness of α-cells that are also exposed to these factors are not fully explored. The development of ER stress is typically followed by an unfolded protein response (UPR) that is mediated by three transmembrane stress sensor proteins: PKR-like ER kinase (PERK), inositol-requiring enzyme 1 (IRE1), and activating transcription factor 6 (ATF6) (14–16). IRE1 cleaves the unspliced X-box binding protein 1 (XBP1u), a member of the cAMP-responsive element–binding protein/ATF family of transcription factors, into the highly active spliced form of XBP1 (XBP1s) (17–19). XBP1s promote ER biogenesis and activate the expression of ER chaperone genes that are required for the folding and trafficking of secretory proteins (20–22). Consistent with its critical role in facilitating protein secretion, XBP1 deficiency impairs the development and function of professional secretory cells such as plasma B cells (23) and pancreatic acinar cells (24). Furthermore, a recent study reported that β-cell–specific XBP1-deficient mice (25) exhibit activation of IRE1 and β-cell dysfunction.

In the current study, we interrogated the role of XBP1 in α-cells by creating complementary in vivo (α-cell–specific XBP1 knockout mouse) and in vitro (stable XBP1 knockdown or overexpression α-cell lines) models. We observed that XBP1 deficiency in α-cells increased ER stress without significantly impacting α-cell survival. However, XBP1-deficient α-cells exhibited alterations in the regulation of glucagon secretion in response to insulin due to defective signaling as a consequence of Jun NH_2-terminal kinase (JNK) activation.

RESEARCH DESIGN AND METHODS

Mouse breeding and physiological experiments. We used male mice for all experiments. Mice were housed in pathogen-free facilities and maintained on a 12-h light/dark cycle at the Foster Biomedical Research Laboratory of Brandeis University in Waltham, Massachusetts. All protocols were approved by the Brandeis University Institutional Animal Care and Use Committee and were in accordance with National Institutes of Health (NIH) guidelines. Blood glucose was monitored with a Glucometer (Elite, Bayer), plasma insulin by ELISA (Crystal Chem, Downers Grove, IL), plasma glucagon by radioimmunoprecipitation assay (RIA; Linco, St. Charles, MO), and plasma glucagon-like peptide 1 (GLP-1) by ELISA (Linco). Glucose and insulin tolerance tests were performed as described previously (26). For the pyruvate challenge test, blood glucose was monitored at 15, 30, 60, and 120 min after an intraperitoneal pyruvate injection (2 g/kg body weight).

Islet isolation and islet secretion assay. Islets were isolated from 6-month-old mice, as described previously (26). After 24-h culture in 7 mmol/L glucose, islets were used in secretion assays, as reported earlier (27). Islets were preincubated at 37°C for 30 min in Krebs-Ringer buffer (KRB) supplemented with 5.5 mmol/L glucose, transferred to 1.5-mL tubes (15 islets per sample),

and incubated in 500 μL KRB with 2.2 or 16.7 mmol/L glucose for 1 h at 37°C. At the end of the incubation period, aliquots from each sample were stored at −20°C for glucagon and insulin assays. Islet DNA, glucagon, and insulin were extracted from aliquots of islets, as reported earlier (27). Glucagon and insulin were measured by RIA or ELISA, as described above.

Histological analysis and electron microscopy. Mice were anesthetized, and the pancreas was rapidly dissected and processed, as described previously (26), and immunostained for insulin (Abcam), glucagon (Sigma-Aldrich), and somatostatin (Abcam). Photomicrographs were obtained with a charge-coupled device camera, and the β-cell, α-cell, δ-cell, and total pancreatic area were estimated using ImageJ software. For transmission electron microscopy, islets were processed by the Joslin Advanced Microscopy Core (DRC) Facility, as reported previously (27).

Cell culture. Glucagon-secreting αTC6 cells were cultured as reported previously (6), and experiments were performed using 80–90% confluent cells.

Lentiviral knockdown of XBP1, overexpression, and inducible system of mouse spliced XBP1. Lentiviral vector plasmid for murine XBP1 short hairpin RNA (shRNA) and control nonsilencing (NS) shRNA were purchased from Open Biosystems. Mouse complete spliced XBP1 open reading frame was amplified from αTC6 cDNA, after thapsigargin treatment, using PCR and cloned into pCDH-CMV-MCS-EF1-Puro lentiviral vector (System Biosciences) for overexpression, and SparQ dual promoter lentiviral vector (System Biosciences) for inducible mouse spliced XBP1. We used SparQTM Cumate Switch Inducible Expression System (System Biosciences) for induction of spliced XBP1. Lentivirus particles were generated by following the manufacturer's recommendation (Open Biosystems). αTC6 cells were plated 24 h before viral infection and then incubated with lentivirus for 24 h. For generating stable cell lines, we began selection with 4 μg/mL of puromycin 48 h after infection and maintained selection for ~14 days before experiments. We generated three separate stable cell lines in each group.

SDS-PAGE and Western blotting. Cells were lysed in RIPA buffer, as reported earlier, and total protein concentration was determined using a bicinchoninic acid assay (Pierce) (27). Samples were resuspended in reducing SDS-PAGE sample buffer, boiled, and resolved by SDS-PAGE. Proteins were subsequently transferred onto polyvinylidene difluoride membranes, blocked in blocking buffer (Thermo Scientific), and incubated with primary antibodies overnight at 4°C. XBP1, ATF6, TATA binding protein (TBP), β-actin, C/EBP homologous protein (CHOP), and IR antibodies were from Santa Cruz. Binding immunoglobulin protein (BiP), IRE1α, pPERK, pJNK, JNK, p-insulin receptor substrate 1 (IRS1) (pS307), pAkt (pT308), pAkt (pS473), total Akt, forkhead box O1 (FoxO1), and cleaved caspase 3 antibodies were from Cell Signaling. pIRE1α antibody is from Novus Biologicals. PERK antibody was from Rockland. pIR (pY972) and pIRS1 (pY896) antibodies are from Invitrogen. IRS1 antibody was from Millipore. Relative protein amounts were estimated by ImageJ software.

Cell secretion assays. Cells were preincubated for 30 min at 37°C in KRB with 25 mmol/L glucose. Subsequently, the cells were treated with 1,000 μL KRB containing 0.5, 5.5, or 25 mmol/L glucose in a 12-well plate for 1 h. At the end of the incubation, aliquots from each sample were used for measurement of glucagon by RIA. Then cells were lysed for DNA extraction.

Measurements of cytoplasmic Ca^{2+} concentrations. Cells on coverslips were incubated for 40 min with 2 μmol/L Fura-2 acetoxymethyl ester at 37°C and washed by KRB with 0.5 mmol/L glucose. Experiments were performed as described earlier (28).

Real-time PCR. RNA was extracted from cells using RNeasy Mini Kit (QIAGEN), and 1 μg RNA was used for a reverse transcription step using the high-capacity cDNA Archive Kit (Applied Biosystems). cDNA was analyzed and amplified using the ABI 7900HT system (Applied Biosystems). TBP was used as an internal control. Primers for glucagon: 5′-TGAATTTGAGAGGCATGCTG-3′ (forward) and 5′-TGGTGCTCATCTCGTCAGAG-3′ (reverse) and for TBP: 5′-ACCCTTCAC CAATGACTCCTATG-3′ (forward) and 5′-ATGATGACTGCAGCAAATCGC-3′ (reverse).

Statistical analysis. All data are expressed as means ± SE and were analyzed with an unpaired two-tailed Student *t* test or ANOVA and post hoc tests as appropriate. Differences were considered significant at $P < 0.05$.

RESULTS

α-Cell specific deletion of XBP1 causes glucose intolerance and insulin resistance due to dysregulated glucagon secretion. α-Cell–specific XBP1 knockout (αXBPKO) mice were created by crossing mice carrying the $Xbp1^{flox}$ allele (25,29) with mice expressing Cre recombinase driven by the glucagon promoter (6,30). The efficiency of recombination by Glu-Cre was consistent with our previous report (6), with ~80% of α-cells expressing β-gal (Fig. 1*A*). αXBPKO mice were born normally and did not exhibit abnormalities in the postnatal period. Body weight, nonfasting blood glucose, insulin, and glucagon levels did not show significant differences between groups until age 6 months (Fig. 1*B–E*), when αXBPKO mice exhibited glucose intolerance (Fig. 1*F*) and insulin resistance (Fig. 1*G*). An intraperitoneal injection of glucose failed to suppress glucagon secretion in αXBPKO mice compared with a significant suppression in controls (Fig. 1*H*). Hepatic glucose production after pyruvate injection was also higher in αXBPKO mice compared with controls (Fig. 1*I*). Insulin and plasma GLP-1 levels were not significantly different between groups (Fig. 1*J* and *K*).

To investigate the potential defects in secretory function, independent of systemic signals, we examined hormone secretion from freshly isolated islets. As expected, exposure of control islets to high glucose (16.7 mmol/L) suppressed glucagon release compared with low glucose (2.2 mmol/L), whereas glucagon secretion from αXBPKO islets was unaffected by high glucose levels (Fig. 1*L*). However, both groups exhibited a similar insulin secretory response to high glucose stimulation (Fig. 1*M*), and the glucagon and insulin content of isolated islets were not significantly different (Fig. 1*N* and *O*). Taken together, these data suggest that XBP1 deficiency in α-cells leads to dysregulation of glucagon secretion and altered glucose homeostasis.

XBP1 deficiency in pancreatic α-cells promotes ER stress without altering islet architecture. Histomorphometric analyses of pancreatic sections in 6-month-old αXBPKO mice showed normal islet architecture (Fig. 2*A* and *B*), and no significant differences were evident in the relative areas of insulin, glucagon, or somatostatin-positive cells between groups (Fig. 2*C–E*). Evaluation of apoptosis by TUNEL staining and BrdU incorporation into α-cells revealed no differences between groups (data not shown).

To examine whether absence of XBP1 promotes ER stress, we performed ultrastructural analyses of pancreas sections using electron microscopy. α-Cells could be distinguished from β- and δ-cells by their distinct secretory granules (31). In the αXBPKO mouse, the ER was severely dilated in ~70% of α-cells compared with normal architecture in controls (Fig. 2*F* and *G*). These data indicate that XBP1 deficiency promotes ER stress in α-cells.

XBP1 deficiency leads to phosphorylation of IRE1α and activation of JNK. To begin to investigate the mechanisms underlying the phenotype, we generated three independent stable αTC6 cell lines, each with a XBP1 knockdown (αXBPKD) or overexpressing mouse spliced XBP1 (mXBP1s; αXBPOE). Stable expression of shRNA of XBP1 or mXBP1s was achieved using a lentiviral vector to transduce αTC6 cells. Nonsilencing shRNA and empty vector were used as controls for knockdown and overexpression cells, respectively. The effectiveness of knockdown or overexpression of the target protein was confirmed by Western blotting (Fig. 3*A* and *D*). In αXBPKD cells, the expression of XBP1s was reduced by ~85% after thapsigargin treatment compared with controls, and the expression of XBP1s in αXBPOE cells was ~10-fold higher than control cells in the basal state.

Next, we examined the proteins associated with the UPR by Western blotting. As expected, the expression of BiP, a downstream target of XBP1s, was decreased in αXBPKD cells (Fig. 3*B* and *C*). However, pIRE1α, a protein upstream of XBP1, was increased in αXBPKD cells, even

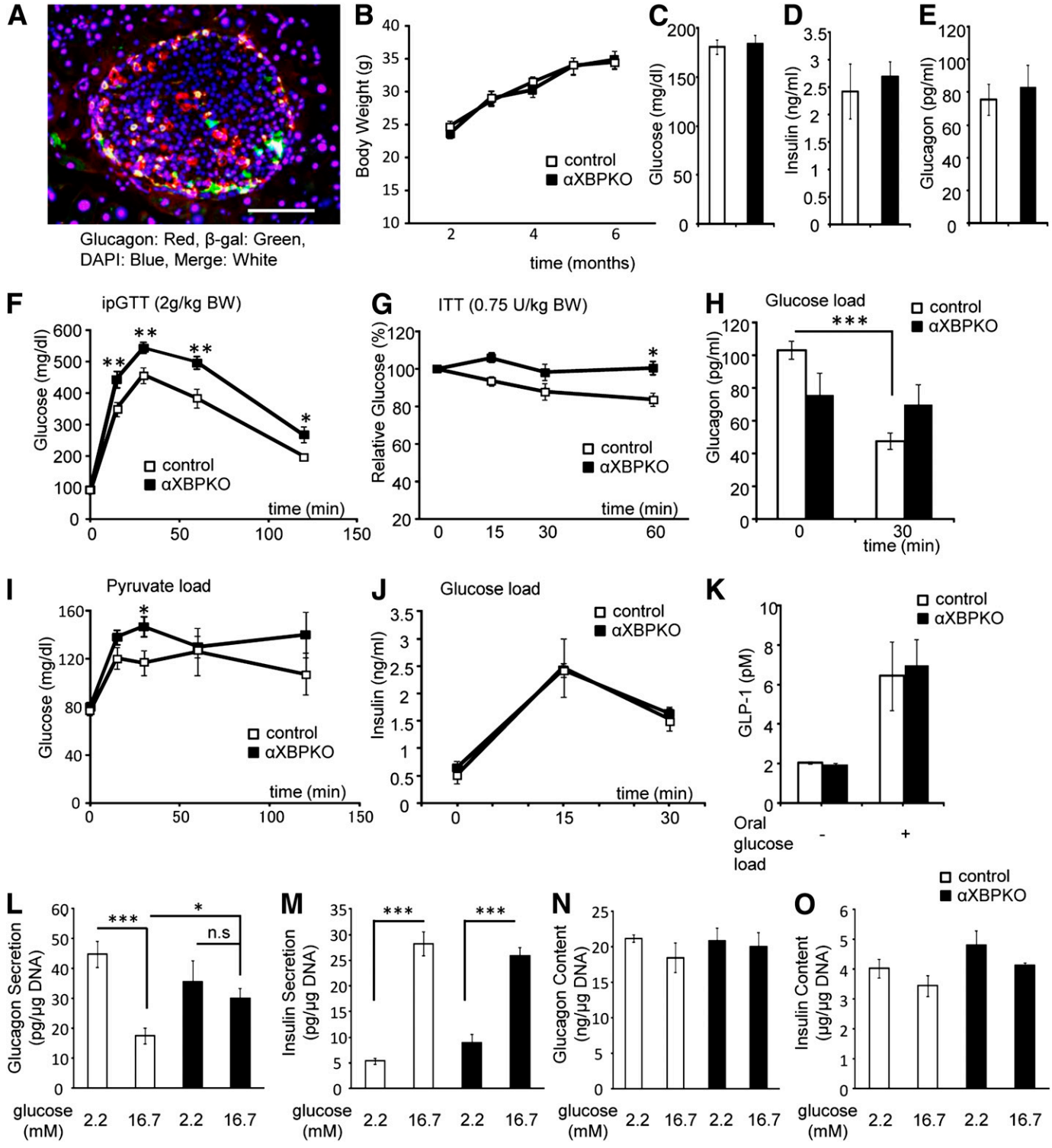

FIG. 1. α-Cell specific deletion of XBP1 promotes glucose intolerance, insulin resistance, and hyperglucagonemia. *A*: Immunofluorescence staining for glucagon (red), β-gal (green), and DAPI (blue) of pancreatic sections from glucagon-Cre/ROSA26-LacZ mice. Scale bar, 100 μm. *B*: Body weights (n = 6–10 in each group). Nonfasting blood glucose (*C*), nonfasting insulin (*D*), and nonfasting glucagon (*E*) in 6-month-old male mice (n = 6 in each group). *F*: Intraperitoneal glucose tolerance test (ipGTT; glucose 2 g/kg body weight [BW]) in 6-month-old male mice (n = 6 in each group). *G*: Whole-body insulin sensitivity by insulin tolerance test (ITT; insulin 0.75 units/kg BW) in 6-month-old male mice (n = 7–11 in each group). *H*: Plasma glucagon levels before and after intraperitoneal glucose injection (glucose 2 g/kg BW) in 6-month-old male mice (n = 7 in each group). *I*: Intraperitoneal pyruvate challenge (pyruvate 2 g/kg BW) in 6-month-old male mice (n = 8–10 in each group). *J*: Plasma insulin levels before and after intraperitoneal glucose injection (glucose 2 g/kg BW) in 6-month-old male mice (n = 7 in each group). *K*: GLP-1 levels before and after oral glucose gavage (at glucose doses 1 g/kg BW; n = 3–4 in each group). Glucagon (*L*) and insulin secretion (*M*) from islets were expressed per microgram of total DNA (n = 3–4 in each group). Total glucagon (*N*), and total insulin (*O*) content of islets expressed per microgram of total DNA (n = 3–4 in each group). Data are expressed as means ± SEM. *P < 0.05, **P < 0.01, ***P < 0.001; n.s., not significant; control vs. αXBPKO.

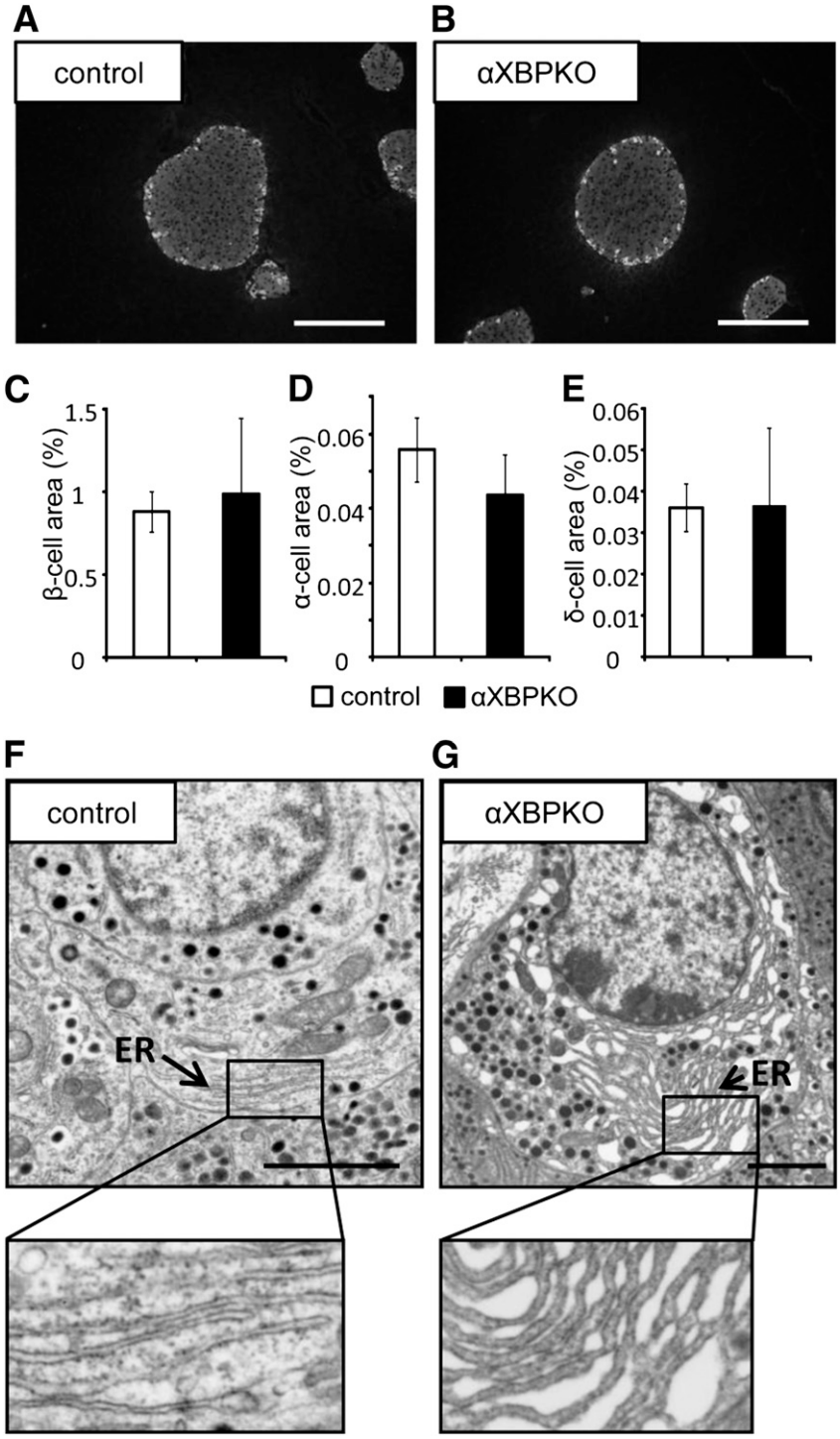

FIG. 2. α-Cell specific deletion of XBP1 causes ER stress but not cell death. Immunofluorescence staining (shown by grayscale) for insulin, glucagon, and somatostatin of pancreatic sections from control mice (*A*) and αXBPKO mice (*B*) at age 6 months (scale bar, 200 μm). Areas positive for insulin (*C*), glucagon (*D*), and somatostatin (*E*) are shown relative to total pancreas at age 6 months (n = 3 in each group) for control and αXBPKO mice. Data are expressed as means ± SEM. Ultrastructural analysis of pancreatic α-cells using electron microscopy was performed on islets from control (*F*) and αXBPKO (*G*) mice at age 6 months (scale bar, 2 μm). The magnification for the enlarged inset is × 43,860 (*F*) and × 32,520 (*G*).

in the basal condition (Fig. 3*B* and *C*). These results confirm the feedback regulation of IRE1α by XBP1 in α-cells, a feature that has been reported in other cell types, including β-cells (25). Examination of other UPR markers revealed increased active ATF6 and reduced pPERK in αXBPKD cells compared with control cells (Fig. 3*A*–*C*). To explore the effects of ER stress on activation of JNK (32), we examined the expression of pJNK in the αXBPKD cells. As expected, pJNK was upregulated in αXBPKD cells compared with controls (Fig. 3*B* and *C*). The expression levels of BiP, pIRE1α, and pJNK in αXBPOE cells were virtually opposite to that observed in αXBPKD cells.

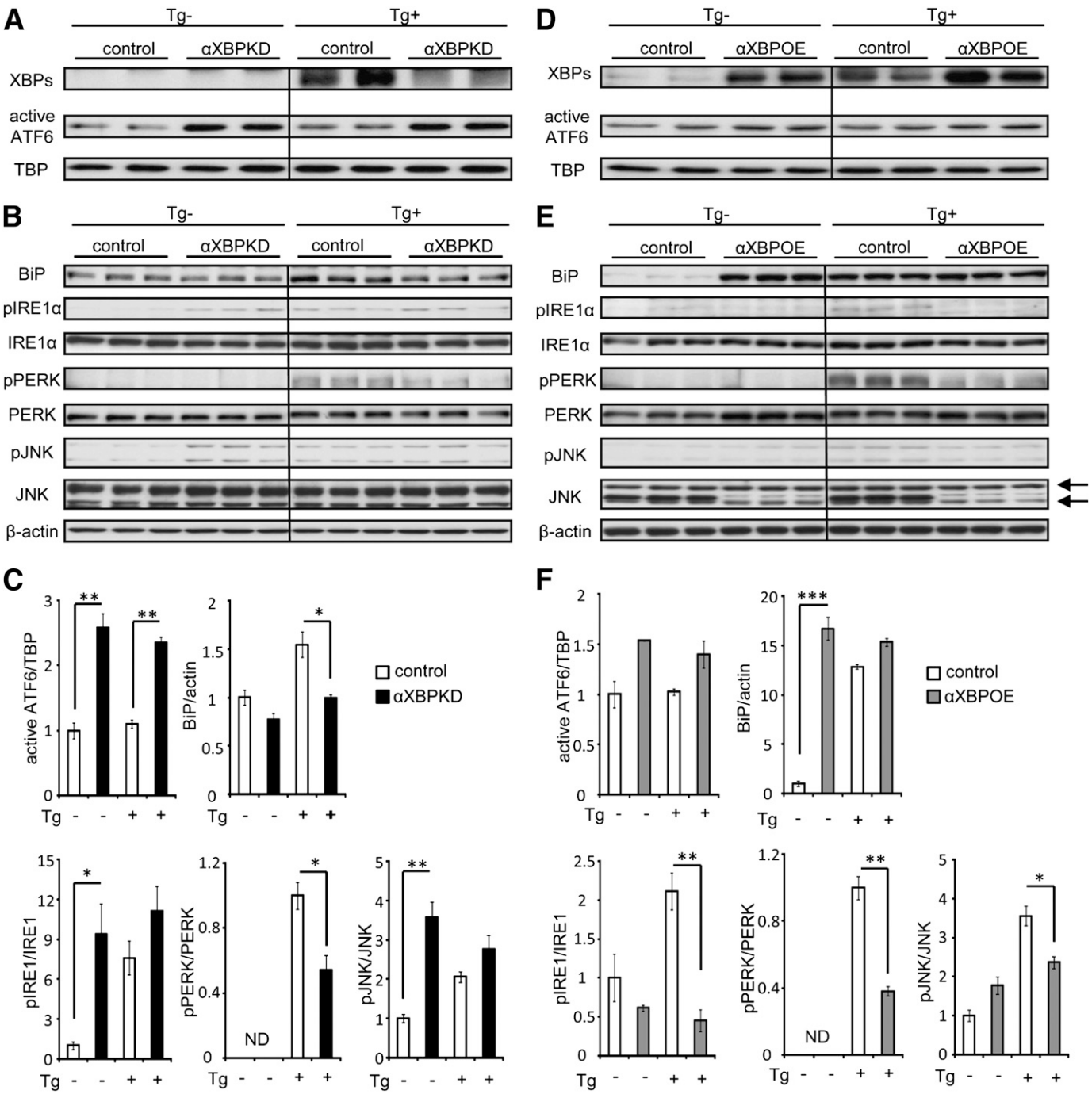

FIG. 3. Activated IRE1α due to XBP1 deficiency leads to activation of JNK. Western blotting for spliced XBP1, active ATF6, and TBP (loading control) in control or αXBPKD cell lines (*A*) and in control or αXBPOE cell lines (*D*) before and after thapsigargin (Tg) treatment for 4 h (100 nmol/L) using nuclear fractions. Western blotting for BiP, pIRE1α, IRE1α, pPERK, PERK, pJNK, JNK, and β-actin (loading control) in control or αXBPKD cell lines (*B*) and in control or αXBPOE cell lines (*E*) before and after thapsigargin (Tg) treatment for 4 h (100 nmol/L). Quantification is shown for active ATF6/TBP, BiP/actin, pIRE1/IRE1, pPERK/PERK, and pJNK/JNK in control or αXBPKD cell lines (*C*) and in control or αXBPOE cell lines (*F*). Data are expressed as means ± SEM. *$P < 0.05$, **$P < 0.01$, ***$P < 0.001$. ND, not detected.

However, active ATF6 and pPERK showed a trend that was similar in αXBPKD and αXBPOE cells compared with their respective controls (Fig. 3*D*–*F*). Taken together, these data suggest feedback mechanisms between XBP1 and IRE1α and that XBP1 deficiency activates IRE1α and phosphorylation of JNK. The alterations in ATF6 and PERK warrant further investigation.

XBP1 deficiency impairs insulin signaling and insulin suppression of glucagon secretion. We next examined the effects of activation of JNK on phosphorylation of IRS1. As expected, IRS1 serine phosphorylation, which has been shown to have a negative effect on IRS1 signaling in some studies (33), was significantly increased in the basal state in αXBPKD cells compared with controls (Fig. 4*A* and *B*). In contrast, IRS1 tyrosine phosphorylation was significantly lower, and consequently, Akt Thr^{308} and Akt Ser^{473} phosphorylation were both markedly decreased in αXBPKD cells after insulin stimulation (Fig. 4*A* and *B*). In

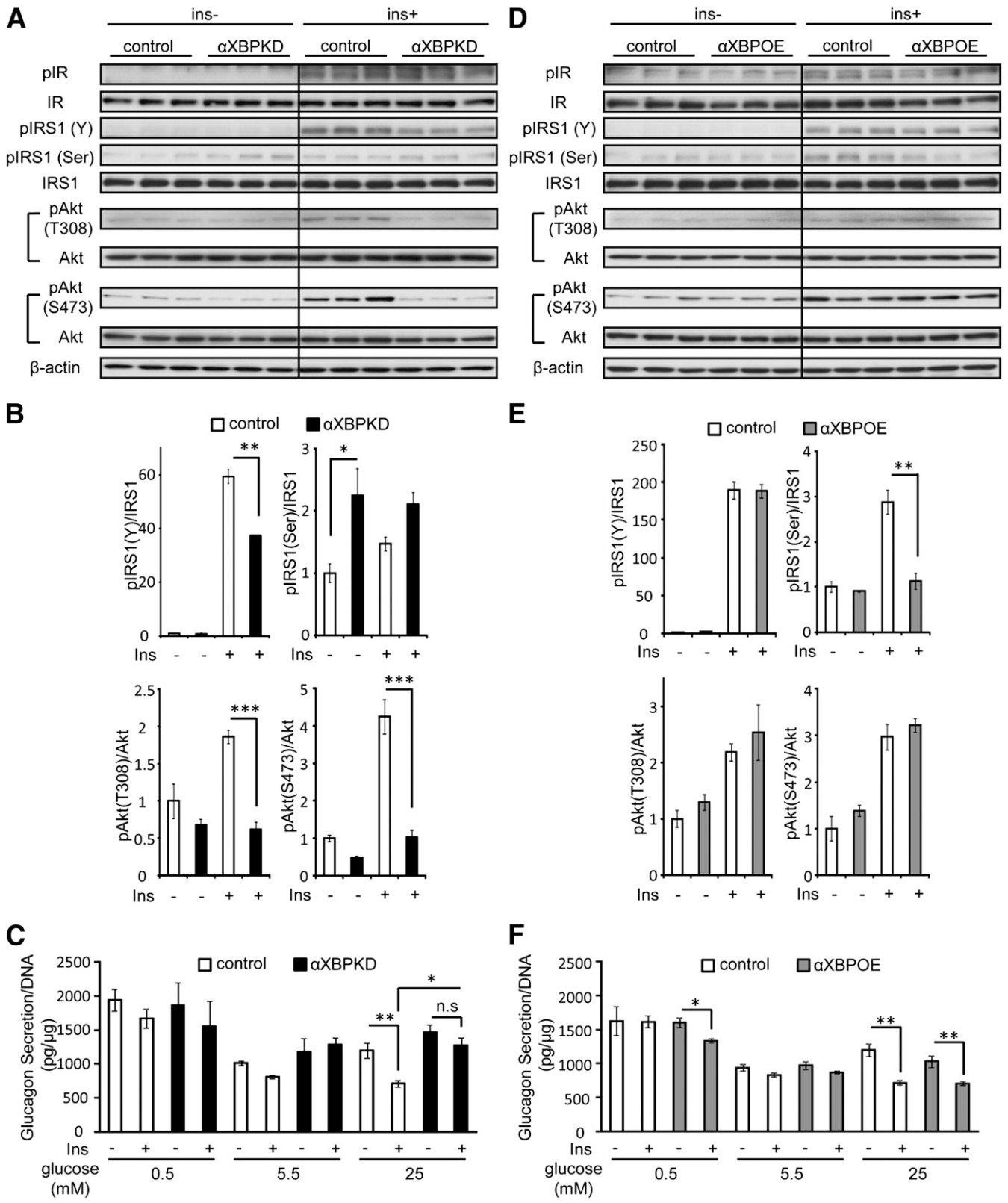

FIG. 4. XBP1 deficiency impairs insulin signaling. Western blotting for insulin receptor (IR) tyrosine^{972} (Y) phosphorylation (pIR), IR, IRS1 tyrosine^{896} (Y) phosphorylation, IRS1 Ser^{307} (Ser) phosphorylation, total IRS1, Akt Thr^{308} phosphorylation, Akt Ser^{473} phosphorylation, total Akt, and β-actin (loading control) in control or αXBPKD cell lines (*A*) and in control or αXBPOE cell lines (*D*) before and after insulin (ins) treatment for 10 min (100 nmol/L). Quantification of pIRS1(Y)/IRS1, pIRS1(Ser)/IRS1, pAkt(T308)/Akt, and pAkt(S473)/Akt in control or αXBPKD cell lines (*B*) and in control or αXBPOE cell lines (*E*). Data are expressed as means ± SEM. *$P < 0.05$, **$P < 0.01$, ***$P < 0.001$. Glucagon secretion from control or αXBPKD cell lines (*C*) and control or αXBPOE cell lines (*F*) was assessed by static incubation for 60 min under various glucose concentrations, without or with 100 nmol/L insulin (Ins), and expressed per microgram of total DNA (n = 3–6 in each group). Data are expressed as means ± SEM. *$P < 0.05$, **$P < 0.01$; n.s., not significant.

αXBPOE cells, however, we observed decreased IRS1 serine phosphorylation after insulin stimulation, although IRS1 tyrosine phosphorylation, Akt Thr^{308} phosphorylation, and Akt Ser^{473} phosphorylation were not significantly different compared with control cells (Fig. 4*D* and *E*).

On the basis of our previous report that impaired insulin signaling in α-cells leads to enhanced glucagon secretion (6), we hypothesized that αXBPKD cells would exhibit an inability to suppress glucagon secretion by insulin. Examination of control cells revealed that glucagon secretion was maximally suppressed at 5.5 mmol/L glucose compared with 0.5 or 25 mmol/L glucose (Fig. 4*C* and *F*). These results are consistent with previous reports showing maximal suppression of glucagon secretion at ~7 mmol/L glucose concentration but paradoxically increased at higher glucose (>10 mmol/L) (34). In addition, insulin in the concentration range between 1 pmol/L and 1 μmol/L has been reported to suppress glucagon secretion from αTC6 cells in the presence of high glucose (25 mmol/L) (35). However, the failure of 100 nmol/L insulin to suppress glucagon secretion in the presence of high glucose (25 mmol/L) suggests impaired insulin signaling in αXBPKD cells (Fig. 4*C*). Glucagon secretion was not significantly different between control and αXBPOE cells (Fig. 4*F*).

Consistent with the data in αXBPKO mouse α-cells, our observation in αXBPKD cells suggests that XBP1 deficiency impairs insulin signaling and induces the inability of insulin to suppress glucagon secretion.

Alterations in cytoplasmic Ca^{2+} in XBP1-deficient α-cells. Next, we measured cytoplasmic Ca^{2+} concentrations ($[Ca^{2+}]$) to assess the mechanism of dysregulation of glucagon secretion in αXBPKD cells. Consistent with previous reports (4,34), cytoplasmic $[Ca^{2+}]$ oscillations in control cells were dampened by application of high glucose and insulin (Fig. 5*A*, *C*, and *F*). A similar trend was evident in αXBPKD cells, although the response was blunted compared with control cells (Fig. 5*A*, *B*, and *F*). However, the average $[Ca^{2+}]$ level in αXBPKD cells when incubated in 0.5 or 25 mmol/L glucose or in 25 mmol/L glucose with 100 nmol/L insulin, was not significantly different from control cells (Fig. 5*A*, *B*, and *E*). On the other hand, the basal $[Ca^{2+}]$ was significantly higher in αXBPOE cells compared with controls, although the $[Ca^{2+}]$ oscillations were similar in the two groups (Fig. 5*C*–*F*). These data suggest that alterations in $[Ca^{2+}]$ are unlikely to underlie the dysregulation of glucagon secretion in XBP1 deficient α-cells. Further studies are warranted to carefully dissect the alterations in $[Ca^{2+}]$ when the expression levels of XBP1 are manipulated.

Chronic XBP1 deficiency in α-cell line leads to decreased glucagon gene expression. Because our experiments in αXBPKD cells suggested a role for XBP1 in the regulation of glucagon secretion, we next examined potential effects at the transcriptional level. Consistent with earlier reports (36,37), glucagon gene expression in control cells was significantly suppressed by insulin at a glucose concentration of 10 mmol/L but not at 2.8 mmol/L (Fig. 6*A* and *B*). In contrast, glucagon gene expression in αXBPKD cells was not suppressed by insulin, although basal glucagon gene expression was lower (Fig. 6*A*). On the other hand, interestingly, the ability of exogenous insulin to inhibit glucagon gene expression was obvious in αXBPOE cells (Fig. 6*B*).

We next examined the expression of nuclear FoxO1 because it has been reported to directly bind the preproglucagon gene promoter and regulate glucagon gene expression (37). In αXBPKD cells, nuclear FoxO1 was already decreased compared with control cells in the basal state, and insulin stimulation did not promote further exclusion of FoxO1 from the nucleus (Fig. 6*C* and *E*). In contrast, stimulation of αXBPOE cells with exogenous insulin had a significant effect on FoxO1 exclusion from the nucleus (Fig. 6*D* and *E*). Together, these data suggest that XBP1 regulates glucagon gene expression via the FoxO1 pathway in α-cells.

Acute induction of spliced XBP1 promotes apoptosis, whereas XBP1 deficiency blocks apoptosis signaling. Histological analyses of pancreas sections from αXBPKO mice showed a normal complement of islet cells, indicating that absence of XBP1 does not enhance α-cell death in the basal state in vivo (Fig. 2). Therefore, we next sought to study the effects of XBP1 on cell growth and apoptosis in our in vitro models. First, examination of growth in αXBPKD and αXBPOE cells did not show significant differences between groups when compared with their respective controls (Fig. 7*A* and *B*). CHOP, a proapoptotic protein induced by ER stress, and active caspase 3 were significantly lower in αXBPKD cells in the basal state and after thapsigargin treatment (Fig. 7*C* and *D*). Surprisingly, αXBPOE cells also exhibited a decrease in CHOP expression after thapsigargin treatment, whereas expression of active caspase 3 was not significantly altered (Fig. 7*E* and *F*). One potential explanation for this conflicting result is that αXBPOE is a stable cell line that expresses high levels of XBP1s. This prompted us to design an experiment to examine the effects of "acute" overexpression of XBP1s by using cumate to induce XBP1s (38). After confirmation of induction of XBP1s by Western blotting (Fig. 8*A*), and consistent with an increased expression of XBP1s, the downstream target BiP was upregulated in the basal state (Fig. 8*B*). Interestingly, CHOP and active caspase 3 expression were both significantly increased after acute induction of XBP1s (Fig. 8*B*). Although there was no difference in the expression of pIRE1α, phosphorylation of JNK was significantly upregulated by acute induction of XBP1s (Fig. 8*B*). The activation of JNK is possibly related to apoptosis induced by acute induction of XBP1s, because JNK is generally activated by various cellular stress pathways (39). The expression of active ATF6 and pPERK after induction of XBP1s showed a trend that was similar to that observed in αXBPOE cells (Fig. 8*A* and *B*). These results from complementary models suggest that acute induction of XBP1s promotes, whereas a knockdown of XBP1 attenuates, apoptosis in α-cells.

DISCUSSION

To directly examine the role of XBP1, a transcription factor that plays a crucial role in the unfolded protein response in pancreatic α-cells, we created and phenotyped mice with a conditional knockout of XBP1 (αXBPKO mice). Here, we report that αXBPKO mice exhibit dysregulation of glucagon secretion and impaired glucose tolerance that is secondary to activation of the IRE1α-JNK pathway and consequent inhibition of IRS1 signaling leading to altered insulin action.

Although impaired glucose utilization due to insulin resistance contributes to the hyperglycemia in patients with T2D, an increase in hepatic glucose production due to altered gluconeogenesis also contributes (40). In normal

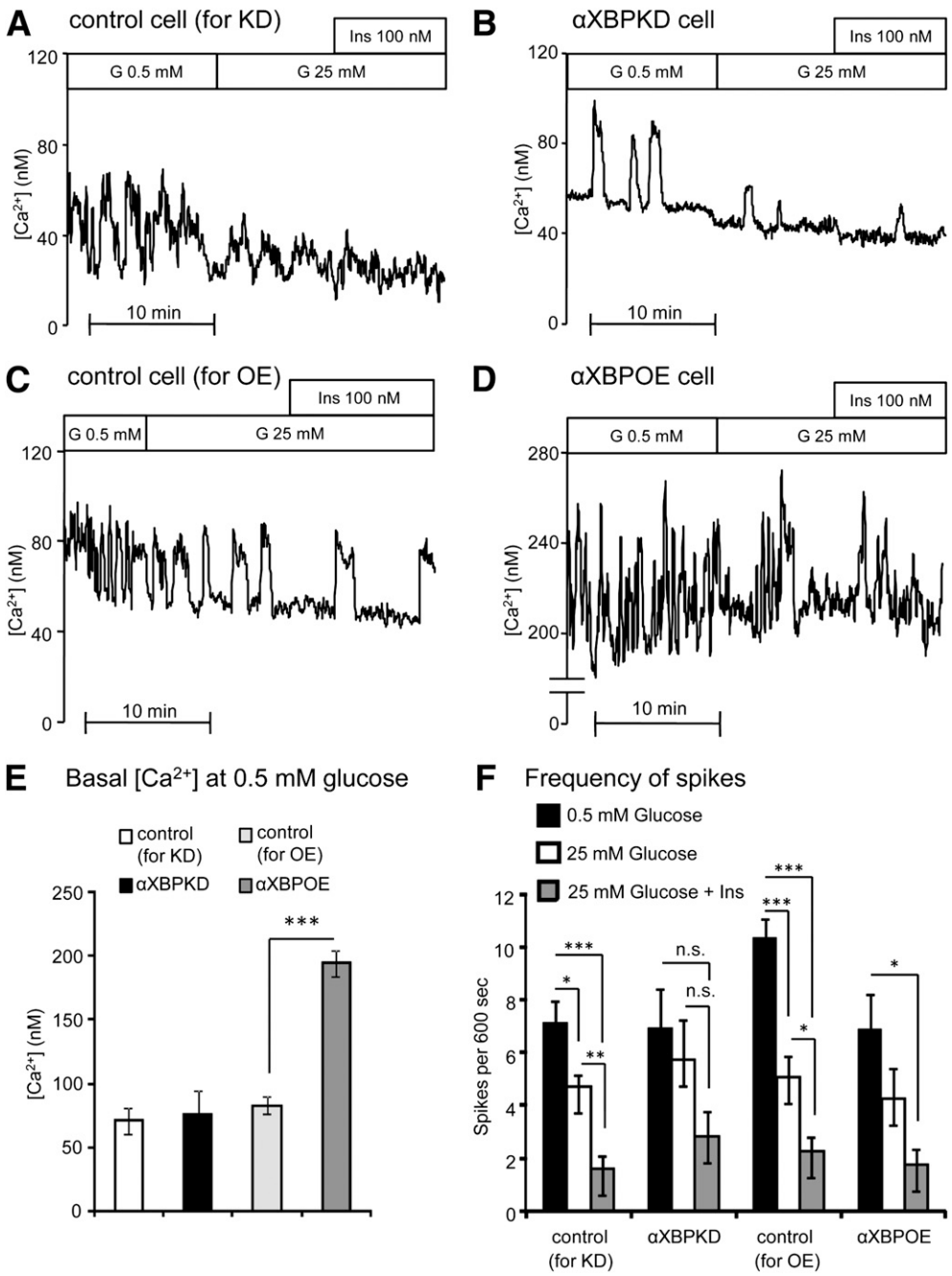

FIG. 5. Effects of altered XBP1 expression on [Ca^{2+}] in αTC6 cells. The glucose (G) concentration was increased from 0.5 to 25 mmol/L, and 100 nmol/L human insulin was present as indicated. Representative traces are shown of single cells from control for KD (*A*), αXBPKD cell (*B*), control for OE (*C*), and αXBPOE cells (*D*). *E*: Basal [Ca^{2+}] is shown for each group (n = 9–15 in each group). Data are expressed as means ± SEM. ***P < 0.0001. *F*: Quantification of frequency of spikes from each group (n = 8–16). Data are expressed as means ± SEM. *P < 0.05, **P < 0.01, ***P < 0.001; n.s., not significant.

subjects, the plasma glucagon concentration falls after oral glucose ingestion, whereas in subjects with T2D, the levels remain high (41), and some patients also exhibit a paradoxical increase in glucagon levels (42). Thus, an inability to suppress glucose production from the liver due to increased glucagon levels is associated with postprandial hyperglycemia in T2D patients. One possible mechanism underlying the hyperglucagonemia in T2D is impaired insulin signaling in α-cells that prevents the appropriate suppression of glucagon secretion. Indeed, mice with functional disruption of insulin receptors in α-cells (αIRKO) exhibit enhanced glucagon secretion and a diabetic phenotype (6). The similar phenotypes of the αXBPKO and αIRKO models support the notion that ER stress in α-cells is linked to altered insulin signaling and contributes to the postprandial hyperglucagonemia in T2D.

Among secretory cells, the β-cell is highly susceptible to ER stress (12,13), which may partly contribute to a significant reduction in β-cell mass in T2D, whereas α-cell mass is relatively normal (10), despite being exposed to high glucose and/or high free fatty acid levels. Our observation that absence of XBP1 did not affect α-cell mass in the αXBPKO mice or cell growth in the αXBPKD cells indicates that α-cells are relatively resistant to ER stress. One

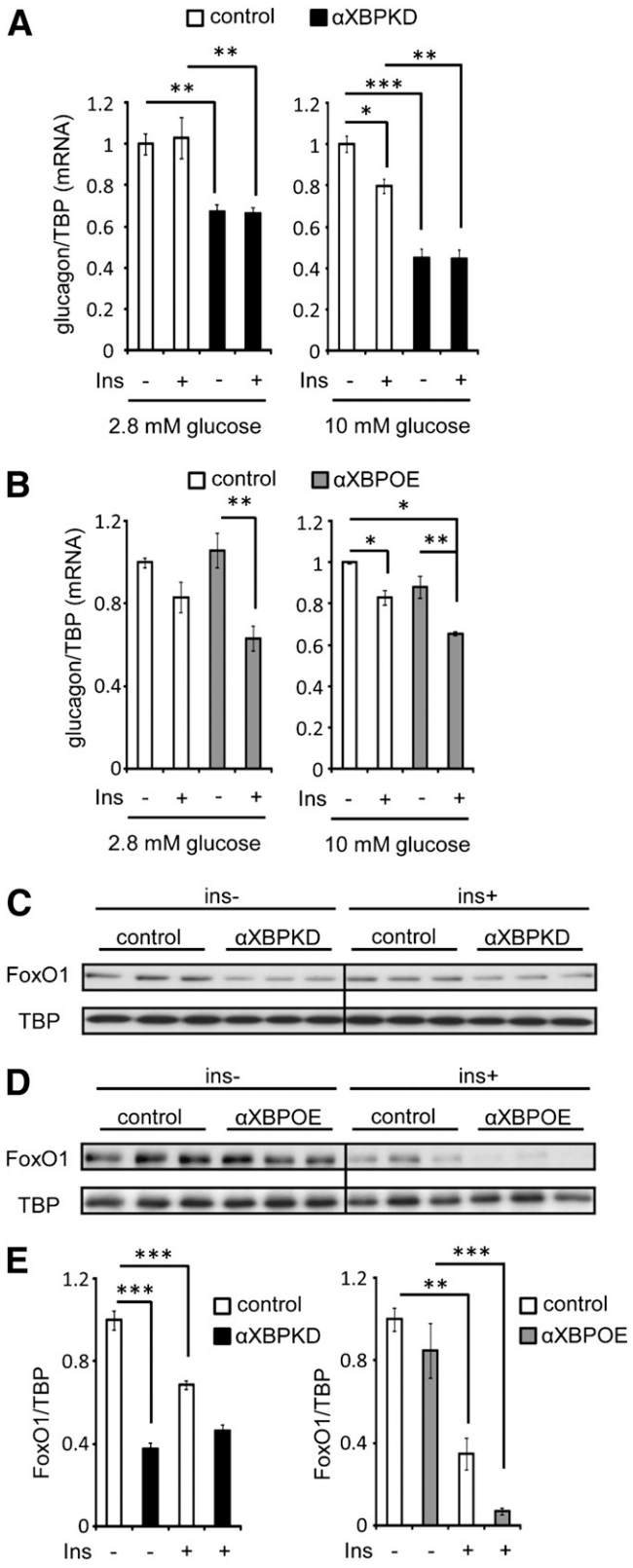

FIG. 6. Effect of XBP1 knockdown or overexpression on glucagon gene expression. Real-time PCR of glucagon gene expression of control or αXBPKD cells (*A*) and control or αXBPOE cells (*B*) incubated at 2.8 and 10 mmol/L glucose concentration with/without 100 nmol/L insulin (Ins) for 6 h. Value were normalized by the level of TBP, and fold-changes were calculated relative to control without insulin (n = 3 in each group). Data are expressed as means ± SEM. *P < 0.05, **P < 0.01, ***P < 0.001. Western blotting for FoxO1 and TBP (loading control) in control or αXBPKD cell lines (*C*) and in control or αXBPOE cell lines (*D*) before and after insulin (ins) treatment for 3 h (100 nmol/L) using nuclear fraction. *E*: Quantification of FoxO1/TBP in control or αXBPKD cell lines and in control or αXBPOE cell lines before and after insulin treatment. Data are expressed as means ± SEM. **P < 0.01, ***P < 0.001.

possible reason that α-cell development and/or survival are unaffected by lack of XBP1 is a relatively lower demand for glucagon secretion compared with insulin. Nevertheless, the selective regulatory effect of XBP1 on hormone secretion but not on cell growth in the α-cell requires further investigation. It is also worth noting that XBP1 plays diverse roles in other cell types. For example, XBP1-deficient lymphoid chimeric mice are completely deficient in normal plasma B cells, although the number of activated B lymphocytes are normal (23), suggesting that XBP1 is required for the terminal differentiation of B lymphocytes to plasma cells. On the other hand, the deletion of XBP1 in pancreatic acinar cells (24) and intestinal Paneth cells (43) promoted death by apoptosis during development. In hepatocytes and salivary gland acinar cells, XBP1 deficiency led to a modest reduction of secretory protein (24,29) but did not result in cell death or any other overt pathology in these cells, suggesting that XBP1 is essential in a small subset of highly secretory cells.

Hepatocytes and adipocytes have both been reported to be susceptible to ER stress in response to obesity and exhibit inhibition of insulin signaling (44), whereas neuronal cells in the brain manifest altered leptin signaling (45). Further, XBP1 deficiency in the liver or adipose tissue induces the activation of IRE1α and of JNK, with a consequent inhibition of insulin signaling (44), a finding that is also evident in the αXBPKD cells. Taken together, our findings suggest that downregulation of PI3K-Akt signaling is associated with unsuppressed glucagon secretion in XBP1-deficient α-cells. However, the recent report that IRS1 serine phosphorylation is beneficial to insulin signaling (46) suggests the effects mediated by the IRS1/JNK pathway are dependent on context and/or cell type. The reduction in nuclear translocation of XBP1s in the livers of obese mice (47) suggests that obesity promotes XBP1s deficiency in hepatocytes. Whether obesity similarly affects other tissues, including α-cells, with consequent defects in dysregulation of glucagon secretion and hyperglucagonemia is not understood and requires investigation.

The lack of a significant alteration in $[Ca^{2+}]$ in αXBPKD cells, despite an increase in glucagon secretion, suggests cAMP is a dominant second messenger in the regulation of glucagon secretion in α-cells (48). Consistent with this possibility, other studies have reported that glucagon secretion at high glucose concentrations does not require elevation of $[Ca^{2+}]$ (34).

The complementary alteration in glucagon gene expression in αXBPKD and αXBPOE cells indicates that XBP1 regulates glucagon gene expression via FoxO1 and is consistent with previous reports in hepatocytes that XBP1 directly interacts with FoxO1 (49). However, the significantly lower basal glucagon gene expression in αXBPKD cells, despite a relatively normal glucagon secretion, suggests the regulation of glucagon translation is independent of mechanisms that modulate gene expression. It is possible that the mammalian target of rapamycin complex 1 pathway, a downstream target of Akt that

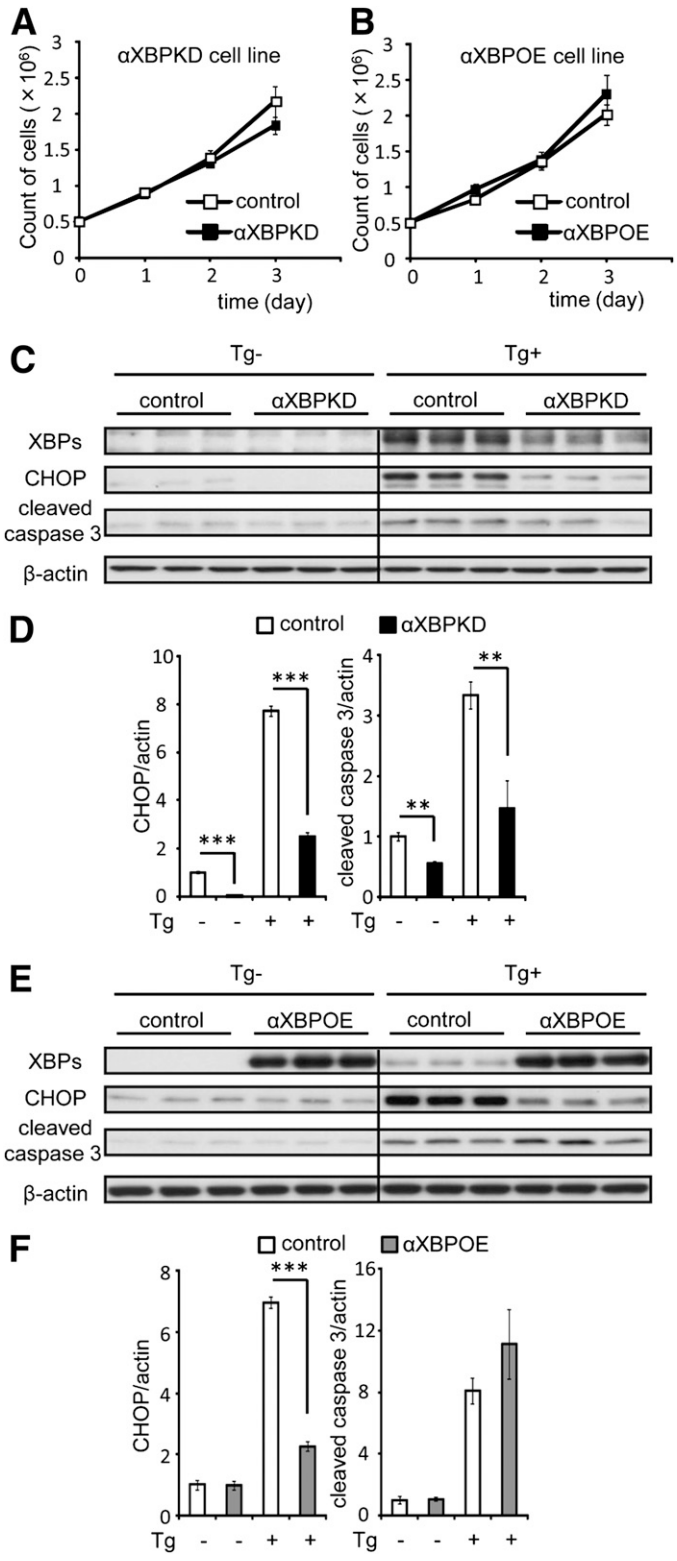

FIG. 7. XBP1 deficiency prevents apoptosis. αXBPKD cells (*A*) or αXBPOE cells (*B*) were plated onto 6-well plates (5×10^5/well) with corresponding controls, and cells were counted on the indicated day. Data are expressed as means ± SEM (n = 4–6 in each group). Western blotting for spliced XBP1, CHOP, cleaved caspase 3, and β-actin (loading control) in control or αXBPKD cell lines (*C*) and in control or αXBPOE cell lines (*E*) before and after thapsigargin (Tg) treatment for 4 h (100 nmol/L). Quantification of CHOP/actin and cleaved caspase 3/actin in control or αXBPKD cell lines (*D*) and in control or αXBPOE cell lines (*F*). Data are expressed as means ± SEM. **$P < 0.01$, ***$P < 0.001$.

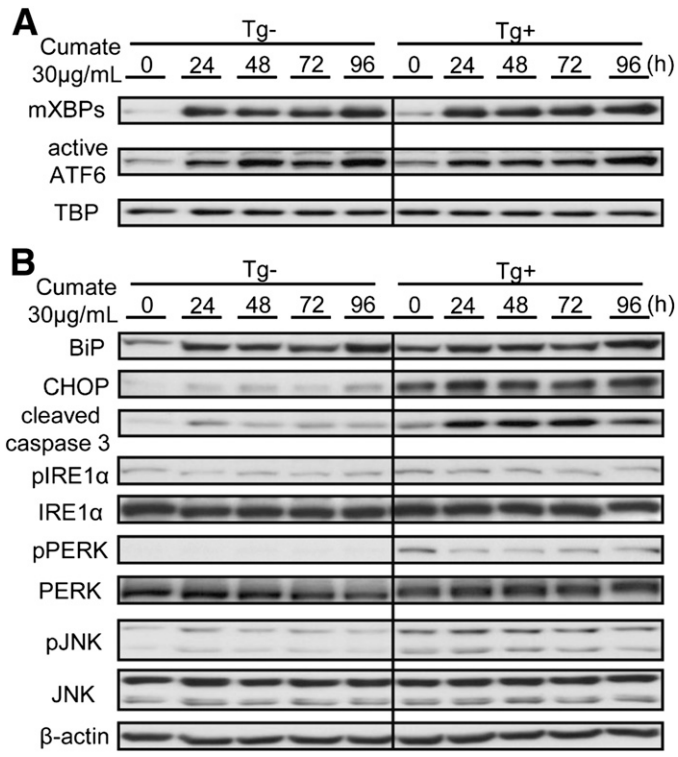

FIG. 8. Acute induction of spliced XBP1 promotes apoptosis. Western blotting for spliced XBP1, active ATF6, and TBP (loading control) using nuclear fraction (*A*), and BiP, CHOP, cleaved caspase 3, pIRE1α, IRE1α, pPERK, PERK, pJNK, JNK, and β-actin (loading control) (*B*) in cells before and after induction of mouse spliced XBP1 by cumate (Cu, 30 μg/mL) without/with thapsigargin (Tg) treatment for 4 h (100 nmol/L). The blot is representative of independent experiments repeated three times.

regulates protein synthesis (50), is involved in this mechanism.

In summary, we report that XBP1 interacts with proteins in the insulin-signaling pathway to regulate glucagon secretion in α-cells. We propose that ER stress in α-cells contributes to hyperglucagonemia and altered glucose homeostasis and that ER chaperones could be used in therapeutic approaches to modify α-cell function in T2D.

ACKNOWLEDGMENTS

Some reagents used in this research work were supported by NIH RO1-DK-67536 (R.N.K.), NIH R37-DK046960 (R.T.K.), and NIH K99-DK090210 (C.W.). M.A. is the recipient of a Research Fellowship from the Hiroo Kaneda Research Aid Fund of the Sunstar Foundation of Osaka, Japan.

No potential conflicts of interest relevant to this article were reported.

M.A. designed and performed research, analyzed data, and wrote the manuscript. C.W.L., J.H., R.M., and B.H. performed research. S.L. and R.T.K. performed the experiment on Ca^{2+} measurements. R.N.K. supervised the project, designed the research, and wrote the manuscript. M.A. and R.N.K. are the guarantors of this work and, as such, had full access to all the data in the study and take responsibility for the integrity of the data and the accuracy of the data analysis.

The authors thank Jonathon N. Winnay, PhD (Joslin), for discussions, Christopher Cahill (Joslin), for assistance with electron microscopy, Laurie Glimcher, PhD (Weill Cornell Medical School, NY), for XBP1 floxed mice, and

Pedro Herrera, PhD (Geneva, Switzerland), for sharing the glucagon-Cre mice.

REFERENCES

1. Reaven GM, Chen YD, Golay A, Swislocki AL, Jaspan JB. Documentation of hyperglucagonemia throughout the day in nonobese and obese patients with noninsulin-dependent diabetes mellitus. J Clin Endocrinol Metab 1987;64:106–110
2. Unger RH, Aguilar-Parada E, Müller WA, Eisentraut AM. Studies of pancreatic alpha cell function in normal and diabetic subjects. J Clin Invest 1970;49:837–848
3. Baron AD, Schaeffer L, Shragg P, Kolterman OG. Role of hyperglucagonemia in maintenance of increased rates of hepatic glucose output in type II diabetics. Diabetes 1987;36:274–283
4. Ravier MA, Rutter GA. Glucose or insulin, but not zinc ions, inhibit glucagon secretion from mouse pancreatic alpha-cells. Diabetes 2005;54:1789–1797
5. Gerich JE, Tsalikian E, Lorenzi M, et al. Normalization of fasting hyperglucagonemia and excessive glucagon responses to intravenous arginine in human diabetes mellitus by prolonged infusion of insulin. J Clin Endocrinol Metab 1975;41:1178–1180
6. Kawamori D, Kurpad AJ, Hu J, et al. Insulin signaling in alpha cells modulates glucagon secretion in vivo. Cell Metab 2009;9:350–361
7. Gerich JE, Lorenzi M, Schneider V, et al. Inhibition of pancreatic glucagon responses to arginine by somatostatin in normal man and in insulin-dependent diabetics. Diabetes 1974;23:876–880
8. Rorsman P, Berggren PO, Bokvist K, et al. Glucose-inhibition of glucagon secretion involves activation of GABAA-receptor chloride channels. Nature 1989;341:233–236
9. Ishihara H, Maechler P, Gjinovci A, Herrera PL, Wollheim CB. Islet beta-cell secretion determines glucagon release from neighbouring alpha-cells. Nat Cell Biol 2003;5:330–335
10. Yoon KH, Ko SH, Cho JH, et al. Selective beta-cell loss and alpha-cell expansion in patients with type 2 diabetes mellitus in Korea. J Clin Endocrinol Metab 2003;88:2300–2308
11. Poitout V, Robertson RP. Glucolipotoxicity: fuel excess and beta-cell dysfunction. Endocr Rev 2008;29:351–366
12. Eizirik DL, Cardozo AK, Cnop M. The role for endoplasmic reticulum stress in diabetes mellitus. Endocr Rev 2008;29:42–61
13. Marchetti P, Bugliani M, Lupi R, et al. The endoplasmic reticulum in pancreatic beta cells of type 2 diabetes patients. Diabetologia 2007;50:2486–2494
14. Schröder M, Kaufman RJ. The mammalian unfolded protein response. Annu Rev Biochem 2005;74:739–789
15. Ron D, Walter P. Signal integration in the endoplasmic reticulum unfolded protein response. Nat Rev Mol Cell Biol 2007;8:519–529
16. Scheuner D, Kaufman RJ. The unfolded protein response: a pathway that links insulin demand with beta-cell failure and diabetes. Endocr Rev 2008;29:317–333
17. Yoshida H, Matsui T, Yamamoto A, Okada T, Mori K. XBP1 mRNA is induced by ATF6 and spliced by IRE1 in response to ER stress to produce a highly active transcription factor. Cell 2001;107:881–891
18. Lee K, Tirasophon W, Shen X, et al. IRE1-mediated unconventional mRNA splicing and S2P-mediated ATF6 cleavage merge to regulate XBP1 in signaling the unfolded protein response. Genes Dev 2002;16:452–466
19. Calfon M, Zeng H, Urano F, et al. IRE1 couples endoplasmic reticulum load to secretory capacity by processing the XBP-1 mRNA. Nature 2002;415:92–96
20. Lee AH, Iwakoshi NN, Glimcher LH. XBP-1 regulates a subset of endoplasmic reticulum resident chaperone genes in the unfolded protein response. Mol Cell Biol 2003;23:7448–7459
21. Shaffer AL, Shapiro-Shelef M, Iwakoshi NN, et al. XBP1, downstream of Blimp-1, expands the secretory apparatus and other organelles, and increases protein synthesis in plasma cell differentiation. Immunity 2004;21:81–93
22. Sriburi R, Jackowski S, Mori K, Brewer JW. XBP1: a link between the unfolded protein response, lipid biosynthesis, and biogenesis of the endoplasmic reticulum. J Cell Biol 2004;167:35–41
23. Reimold AM, Iwakoshi NN, Manis J, et al. Plasma cell differentiation requires the transcription factor XBP-1. Nature 2001;412:300–307
24. Lee AH, Chu GC, Iwakoshi NN, Glimcher LH. XBP-1 is required for biogenesis of cellular secretory machinery of exocrine glands. EMBO J 2005;24:4368–4380
25. Lee AH, Heidtman K, Hotamisligil GS, Glimcher LH. Dual and opposing roles of the unfolded protein response regulated by IRE1alpha and XBP1 in proinsulin processing and insulin secretion. Proc Natl Acad Sci U S A 2011;108:8885–8890
26. Kulkarni RN, Brüning JC, Winnay JN, Postic C, Magnuson MA, Kahn CR. Tissue-specific knockout of the insulin receptor in pancreatic beta cells creates an insulin secretory defect similar to that in type 2 diabetes. Cell 1999;96:329–339
27. Liew CW, Bochenski J, Kawamori D, et al. The pseudokinase tribbles homolog 3 interacts with ATF4 to negatively regulate insulin exocytosis in human and mouse beta cells. J Clin Invest 2010;120:2876–2888
28. Kulkarni RN, Roper MG, Dahlgren G, et al. Islet secretory defect in insulin receptor substrate 1 null mice is linked with reduced calcium signaling and expression of sarco(endo)plasmic reticulum Ca2+-ATPase (SERCA)-2b and -3. Diabetes 2004;53:1517–1525
29. Lee AH, Scapa EF, Cohen DE, Glimcher LH. Regulation of hepatic lipogenesis by the transcription factor XBP1. Science 2008;320:1492–1496
30. Herrera PL. Adult insulin- and glucagon-producing cells differentiate from two independent cell lineages. Development 2000;127:2317–2322
31. Vantyghem MC, Kerr-Conte J, Pattou F, et al. Immunohistochemical and ultrastructural study of adult porcine endocrine pancreas during the different steps of islet isolation. Histochem Cell Biol 1996;106:511–519
32. Urano F, Wang X, Bertolotti A, et al. Coupling of stress in the ER to activation of JNK protein kinases by transmembrane protein kinase IRE1. Science 2000;287:664–666
33. Hirosumi J, Tuncman G, Chang L, et al. A central role for JNK in obesity and insulin resistance. Nature 2002;420:333–336
34. Salehi A, Vieira E, Gylfe E. Paradoxical stimulation of glucagon secretion by high glucose concentrations. Diabetes 2006;55:2318–2323
35. Kisanuki K, Kishikawa H, Araki E, et al. Expression of insulin receptor on clonal pancreatic alpha cells and its possible role for insulin-stimulated negative regulation of glucagon secretion. Diabetologia 1995;38:422–429
36. Philippe J. Glucagon gene transcription is negatively regulated by insulin in a hamster islet cell line. J Clin Invest 1989;84:672–677
37. McKinnon CM, Ravier MA, Rutter GA. FoxO1 is required for the regulation of preproglucagon gene expression by insulin in pancreatic alphaTC1-9 cells. J Biol Chem 2006;281:39358–39369
38. Mullick A, Xu Y, Warren R, et al. The cumate gene-switch: a system for regulated expression in mammalian cells. BMC Biotechnol 2006;6:43
39. Kyriakis JM, Banerjee P, Nikolakaki E, et al. The stress-activated protein kinase subfamily of c-Jun kinases. Nature 1994;369:156–160
40. Unger RH, Orci L. The role of glucagon in the endogenous hyperglycemia of diabetes mellitus. Annu Rev Med 1977;28:119–130
41. Ohneda A, Watanabe K, Horigome K, Sakai T, Kai Y, Oikawa S. Abnormal response of pancreatic glucagon to glycemic changes in diabetes mellitus. J Clin Endocrinol Metab 1978;46:504–510
42. Mitrakou A, Kelley D, Veneman T, et al. Contribution of abnormal muscle and liver glucose metabolism to postprandial hyperglycemia in NIDDM. Diabetes 1990;39:1381–1390
43. Kaser A, Lee AH, Franke A, et al. XBP1 links ER stress to intestinal inflammation and confers genetic risk for human inflammatory bowel disease. Cell 2008;134:743–756
44. Ozcan U, Cao Q, Yilmaz E, et al. Endoplasmic reticulum stress links obesity, insulin action, and type 2 diabetes. Science 2004;306:457–461
45. Ozcan L, Ergin AS, Lu A, et al. Endoplasmic reticulum stress plays a central role in development of leptin resistance. Cell Metab 2009;9:35–51
46. Copps KD, Hancer NJ, Opare-Ado L, Qiu W, Walsh C, White MF. Irs1 serine 307 promotes insulin sensitivity in mice. Cell Metab 2010;11:84–92
47. Park SW, Zhou Y, Lee J, et al. The regulatory subunits of PI3K, p85alpha and p85beta, interact with XBP-1 and increase its nuclear translocation. Nat Med 2010;16:429–437
48. Tian G, Sandler S, Gylfe E, Tengholm A. Glucose- and hormone-induced cAMP oscillations in α- and β-cells within intact pancreatic islets. Diabetes 2011;60:1535–1543
49. Zhou Y, Lee J, Reno CM, et al. Regulation of glucose homeostasis through a XBP-1-FoxO1 interaction. Nat Med 2011;17:356–365
50. Hay N, Sonenberg N. Upstream and downstream of mTOR. Genes Dev 2004;18:1926–1945